International Journal of Remote Sensing
Vol. 000, No. 000, 0 Month 2005, 1–19

Taylor & Francis
Taylor & Francis Group

Toward aerosol optical depth retrievals over land from GOES visible radiances: determining surface reflectance

K. R. KNAPP*†, R. FROUIN‡, S. KONDRAGUNTA§ and A. PRADOS¶
†NOAA/NCDC/RSAD, 151 Patton Avenue, Asheville, North Carolina 28806, USA
‡Scripps Institution of Oceanography, University of California San Diego, La Jolla, California, USA
§NOAA/ORA, Camp Springs, Maryland, USA
¶CSU/CIRA, Camp Springs, Maryland, USA

(*Received 24 June 2004; in final form 1 February 2005*)

Frequent observations of aerosol over land are desirable for aviation, air pollution and health applications, thus a method is proposed here to correct surface effects and retrieve aerosol optical depth using visible reflectance measurements from the Geostationary Operational Environmental Satellite (GOES). The surface contribution is determined from temporal compositing of visible imagery, where darker pixels correspond to less atmospheric attenuation and surface reflectance is deduced from the composite using radiative transfer. The method is applied to GOES-8 imagery over the eastern US. Retrieved surface reflectance is compared with separate retrievals using *a priori* ground-based observations of aerosol optical depth. The results suggest that surface reflectances can be determined to within ± 0.04. The composite-derived surface reflectance is further analysed by retrieving aerosol optical depth and validating retrievals with Aerosol Robotic Network (AERONET) observations. This analysis indicates that the retrieved optical depth is least biased, hence the surface reflectance is most accurate, when the composite time period varies seasonally. Aerosol optical depth retrievals from this validation are within ± 0.13 of AERONET observations and have a correlation coefficient of 0.72. While aerosol optical depth retrieval noise at low optical depths may be limiting, the retrieval accuracy is adequate for monitoring large outbreaks of aerosol events.

1. Introduction

Aerosols play an important role in numerous aspects of human life. Aerosols have large-scale effects, such as their impact on climate by redistributing solar radiation (Herman and Browning 1975, Charlson *et al.* 1991, Haywood *et al.* 1999) and interacting with clouds (Platnick and Twomey 1994, Kaufman *et al.* 2002). The magnitude of these effects on the Earth's radiation budget, however, is still uncertain (Haywood and Boucher 2000, IPCC 2001). But, aerosols have a 1
significant impact on human life beyond the climate element. In general, average aerosol optical depths are low, for instance they average less than 0.1 for most of the US (Koepke *et al.* 1997, Hess *et al.* 1998). During aerosol outbreaks, however, aerosol optical depths can be much larger. For instance when smoke from fires in

*Corresponding author. Email: Ken.Knapp@noaa.gov; Tel: 828-271-4339; fax: 828-271-4328

International Journal of Remote Sensing
ISSN 0143-1161 print/ISSN 1366-5901 online © 2005 Taylor & Francis Ltd
http://www.tandf.co.uk/journals
DOI: 10.1080/01431160500099329

Central America were transported over the US in May 1998, visibilities were decreased as far north as Minnesota and optical depths (at 0.55 μm) in Kansas were above 2 (Peppler *et al*. 2000). During such events, high aerosol concentrations have detrimental effects on respiratory-sensitive groups (by increasing particulate mass (PM) concentrations) and decrease visibility, affecting aviation and protected environments such as national parks. In these cases, it is not the average aerosol amount that is important, but the timely observation of aerosol events with large optical depths.

In spite of advances in aerosol remote sensing over land (aptly summarized by Kaufman *et al*. 1997 and King *et al*. 1999), most retrievals are limited to twice per day, as by the morning and afternoon passes of the polar orbiting satellites. Aerosols, however, show diurnal variations that would be missed by such sparse observations. While studies of aerosol optical depth from Sun photometers show little systematic trends (Kaufman *et al*. 2000, Smirnov *et al*. 2002), surface observations of scattering show significant diurnal patterns (Bergin *et al*. 2001, Gebhart *et al*. 2001, Xu *et al*. 2002). The Environmental Protection Agency (EPA), in particular, needs to understand aerosol plume movement to track and forecast plume movement in the interest of human health. Therefore, it is important to monitor the temporal aspects of aerosol.

The Geostationary Operational Environmental Satellite (GOES) series has the potential to provide aerosol observations over land and ocean with multiple observations per day. Early studies (Koepke and Quenzel 1979, Fraser *et al*. 1984) demonstrated an ability to perform the retrievals, although the results were limited to case studies. Their sensitivity studies, however, concluded that retrievals depend on aerosol optical property assumptions and surface reflectance.

Studies using newer geostationary satellites (e.g. GOES-8) and larger validation networks (e.g. Aerosol Robotic Network—AERONET) supported those initial findings. Specifically, Zhang and Christopher (2002) and Knapp *et al*. (2001) showed that aerosol monitoring from GOES is possible for South America. However, this region has optimal retrieval conditions: surface cover with little variability (i.e. rainforest) and large aerosol optical depths (from biomass burning). Herein, this paper will investigate conditions are not as optimal as in South America, but where the aerosol burden and surface are more variable: North America. 2

Knapp (2002) showed that there is an aerosol signal in GOES data over North America but did not attempt to perform aerosol optical depth retrievals. The study found strong correlations between surface observed aerosol optical depths and GOES visible reflectances for most regions of the US and for most times of the day. This is significant given the larger range of aerosol types, surface cover, and view zenith angles in North America.

The presence of an aerosol signal, however, does not necessarily imply that aerosol optical depth is retrievable. To retrieve aerosols, one must separate the surface contribution to the satellite reflectance from the atmospheric contribution; that is, one must estimate surface reflectance. Knapp (2002) determined the surface reflectance by correlating satellite reflectance with *in situ* observations of aerosol optical depth (much like determining the solar constant with a Langley plot), thus separating the atmospheric component from the surface. This empirical method is limited to sites with ground-based aerosol optical depth observations. However, the current study attempts to separate the two effects without *in situ* measurements.

Herein, ground-based aerosol optical depth observations are primarily used to test how well the surface effect is removed. Only when this step is successful can the aerosol optical depth be deemed retrievable.

2. Estimating surface contribution

2.1 *The GOES/imager visible observations*

The GOES-8 imager is used herein to perform the surface reflectance and aerosol optical depth (τ) retrievals and mask for clouds. It measures top of the atmosphere (TOA) radiance in five channels: three at infrared wavelengths, one in the visible wavelength and one sensitive to both solar and Earth-emitted radiance. Primarily, the visible channel (0.52–0.72 μm full width at half maximum) is sensitive to aerosol scattering, so the remaining channels are used for cloud masking. The cloud mask algorithm is based on the Clouds from Advanced Very High Resolution Radiometer (AVHRR) (CLAVR) algorithm (Stowe *et al.* 1999) which uses spectral and spatial thresholds to test for the presence of clouds. The visible channel data for this study are subsampled to 4 km resolution at 1 h intervals. This study includes GOES data from the 2001 calendar year, so evaluation for a full annual cycle is possible.

The GOES imager visible sensor has no onboard calibration source, so one must rely on vicarious calibration. The visible observations (DN) are converted to satellite-detected reflectance (ρ_{sat}) according to (Knapp and Vonder Haar 1999):

$$\rho_{sat} = \frac{1}{\delta(d)\mu_o}\frac{DN - C_o}{\gamma} \tag{1}$$

where C_o represents the offset (~29 counts), μ_o is the cosine of the solar zenith angle, δ is the Earth–Sun distance correction factor on day of year (d) and γ is the calibration coefficient. For this study, γ is calculated as:

$$\gamma = 790.4\left[1 + 1.695 \times 10^{-4} D_L\right]^{-1} \tag{2}$$

where D_L is the number of days since the launch of the satellite. This represents a degradation of 4.2% during 2001, determined from a recent analysis by the National Oceanic and Atmospheric Administration (NOAA) to calibrate the GOES sensors (F. Wu, personal communication 2003).

2.2 *Temporal compositing*

Estimating the surface contribution to the TOA GOES visible reflectance is difficult since observations will have atmospheric contamination. For instance, a visible observation from GOES on a cloudless day with low aerosol burden will still have: gaseous absorption (primarily, ozone and water vapour); Rayleigh scattering; and residual aerosol extinction. This atmospheric component to the TOA reflectance needs to be removed to retrieve the surface reflectance. While studies have shown it is possible to estimate the surface component from observations in the near-infrared (e.g. 2.1 μm) where aerosol and Rayleigh scattering are very low (Kaufman and Remer 1994), the GOES imager lacks an observation at this wavelength. Therefore, a compositing method is used to estimate the surface reflectance.

The composite reflectance method uses observations for a given Earth location over a number of days to determine the surface contribution. Clouds increase the TOA reflectance so darker observations correspond to days with less cloud. In

general, aerosols increase the satellite-measured reflectance, but may decrease it given bright surfaces or absorbing aerosol. Thus, the darkest reflectance in time will generally have the least aerosol influence. However, satellite reflectance also depends on illumination geometry due to non-Lambertian surface and Rayleigh scattering. So, a separate composite reflectance is compiled for each time of day.

Cloud shadows, however, can contaminate the composite reflectance. At high solar zenith angles (i.e. during early morning and late afternoon), high clouds will cast large shadows. In the shadow regions, the direct downward solar radiance is obscured at the surface, thereby reducing the surface reflectance. The second darkest observation is used in the composite clear reflectance (CCR) method to reduce the effect of cloud shadows. By selecting the second darkest pixel, a cloud shadow would need to be present on at least two days during the period to affect the composite. Figure 1 shows the darkest (figure 1(*a*)) and second darkest (figure 1(*b*)) composite reflectances for the eastern Nebraska and South Dakota. The composite is from 20 days ending on 18 June 2002; all images are at 12:45 UTC, having a mean solar zenith angle of 71°. Cloud shadows (dark blotches in figure 1(*a*)) are apparent in the darkest reflectance, but are less apparent in the composite of second darkest pixels. The histograms (figure 1(*c*)) of the images show that the number of darker observations (e.g. below 50 digital counts) is larger for the composite of darkest pixels. The composite using the second darkest pixels is used to minimize the presence of cloud shadows.

The accuracy of the composite depends on the length of time used to create it. For instance, enough cloud-free observations must exist with little aerosol influence for the surface reflectance to be accurate. Areas of persistent aerosol or cloud cover will likely have errors in the retrieved surface reflectance because the atmospheric component remains large in such situations. For example, in South America during the biomass burning season, the smoke pall can be present for a month or longer (depending on circulation patterns and amount of burning (Prins *et al.* 1998)). In such instances, the unaccounted atmospheric component causes the retrieved surface reflectance to be too large, thereby causing aerosol optical depth retrievals to be too low. More observations increase the chance of observing a cloud-free, aerosol-free day, but if too many days of observations are used, the surface reflectance may change. For short time scales, surface reflectance is affected by surface moisture changes. This is particularly true for regions with bare soils, such as deserts. However, retrievals herein are primarily over vegetated regions where short-term changes in soil moisture (e.g. from precipitation) have a smaller effect. At longer time scales, the surface reflectance will change with the seasonal growth of vegetation. If the composite period is too long, the surface reflectance will be biased low because more observations provide more opportunities for darker observations. This causes aerosol optical depth retrievals to have a positive bias. A sensitivity study is performed herein to determine the optimal composite length (see §3) to minimize this bias.

2.3 *Atmospheric correction*

Atmospheric effects—aerosol extinction, Rayleigh scattering and gaseous absorption—are removed from the composite using the second simulation of the satellite signal in the solar spectrum (6S) radiative transfer model (Vermote *et al.* 1997a). This retrieves the surface reflectance, ρ_{sfc}. The National Center for Environmental Prediction (NCEP) reanalysis column water vapour and Total Ozone Mapping

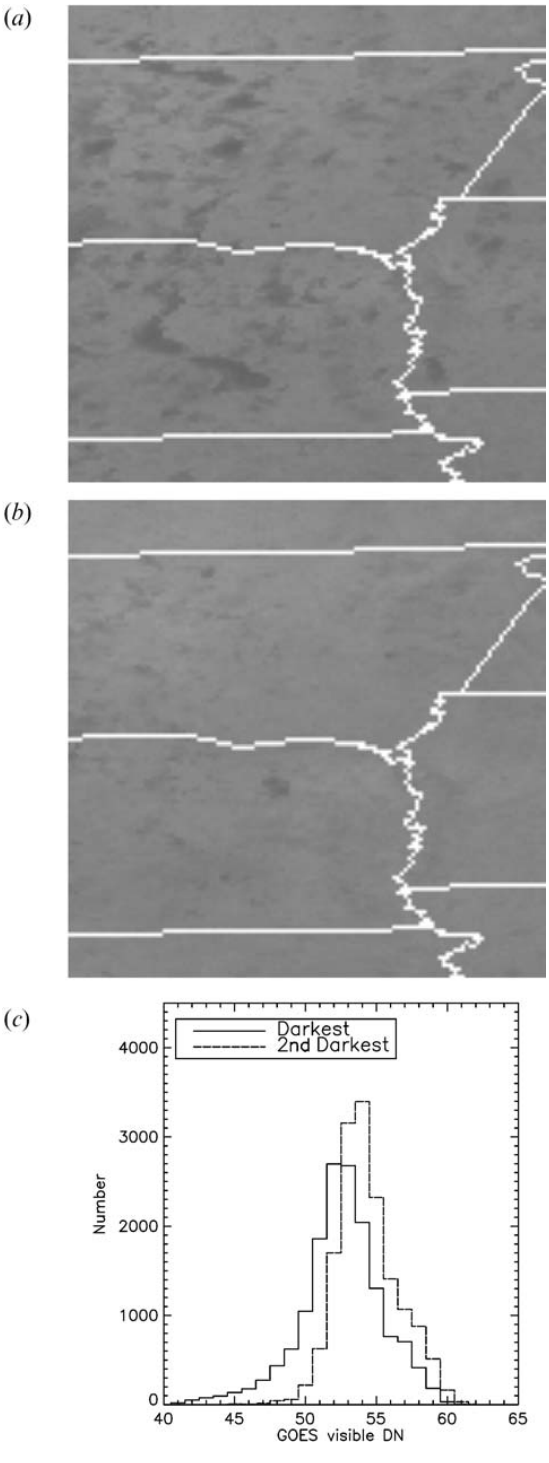

Figure 1. (*a*) Cloud shadows are noticeable in the darkest pixel composite of GOES visible imagery for eastern Nebraska and South Dakota. (*b*) Fewer shadows are present in the composite of the 2nd darkest observation of each pixel. (*c*) The histograms (number of observations per DN) for each image, showing a decrease in the number of observations less than 50 DN for the composite of the 2nd darkest observations.

Spectrometer (TOMS) column ozone are used to correct for absorption. Altitude data from the National Geophysical Data Center TerrainBase dataset is used to estimate the Rayleigh scattering using the US standard atmosphere (McClatchey *et al*. 1972). Surface reflectance is simulated using a Lambertian surface. While the observed land surfaces are not Lambertian, the largest errors (roughly 20%) in the assumption are geometrically limited to regions near the 'hot spot' (Vermote *et al*. 1997b, Knapp *et al*. 2002). However, the bulk of observations from geostationary satellites are geometrically far from the 'hot spot' where errors in this assumption are much less.

Some aerosols are still present in the composite reflectance; their radiative effect must be removed as well. This aerosol is simulated using the continental aerosol model (Lenoble and Brogniez 1984), given its ability to simulate the aerosol signal over the US (Knapp 2002). The continental aerosol model has a single scattering albedo of 0.92, which is similar to values observed during the Tropospheric Aerosol Radiative Forcing Observation Experiment (TARFOX) (Hegg *et al*. 1997). This will represent the aerosol extinction still present in a composite reflectance. The amount of background aerosol is difficult to determine because it varies with season, length of CCR and time of day. Therefore, the following sensitivity study has been done to determine the appropriate background aerosol optical depth, τ_b.

2.4 *Evaluation methods*

Given the need to determine the optimal composite length and τ_b to retrieve surface reflectance, it is necessary to evaluate the surface reflectance estimates. Herein, two approaches are used which use ground-based aerosol optical depth observations. First, consider the simple situation where the satellite reflectance, ρ_{sat}, is only a function of aerosol optical depth,τ, and surface reflectance, ρ_{sfc}:

$$\rho_{sat} = f(\tau, \rho_{sfc}) \tag{3}$$

This ignores important radiative transfer parameters which are either fixed (e.g. geometry), corrected (e.g. gaseous absorption), or assumed (e.g. aerosol optical properties). One could compare the surface reflectance retrieved from the composite image ($\rho_{sfc,CCR}$):

$$\rho_{sfc,CCR} = f^{-1}\left(\tau_b, \rho_{sat,CCR}\right) \tag{4}$$

with a surface reflectance retrieved from an instantaneous satellite observation (ρ_{sat}) and an observed optical depth ($\rho_{sfc,AER}$):

$$\rho_{sfc,AER} = f^{-1}\left(\tau_A, \rho_{sat}\right) \tag{5}$$

where, τ_b is the estimated aerosol optical depth contributing to $\rho_{sat,CCR}$ (the composite clear reflectance) and τ_A is the ground-based AERONET optical depth contributing to ρ_{sat}. The same continental aerosol model is used in the $\rho_{sfc,AER}$ retrieval. The $\rho_{sfc,AER}$ has uncertainty due to differences between the assumed (continental) and actual aerosol optical properties, and to surface reflectance anisotropy, neglected in the inversion of ρ_{sat}.

For the second approach, the ability to estimate surface reflectances is evaluated by validating the ensuing aerosol optical depth retrievals. In doing so, one can determine if the surface effect is satisfactorily removed. In essence, it compares

aerosol optical depth from AERONET level 2.0, τ_A, with retrieved optical depth, τ_G:

$$\tau_G = f^{-1}\left[\rho_{sat}, f^{-1}\left(\tau_b, \rho_{sat,CCR}\right)\right] \quad (6)$$

In this instance, the ground-based observation is of high quality (error is less than ± 0.02 according to Holben *et al*. 1998) with retrieval uncertainty isolated in the τ_G parameter. That is, both the atmospheric correction and aerosol retrieval uncertainty affect τ_G. These approaches are used below to evaluate the ability to separate the surface from the atmospheric component in GOES visible reflectances.

Other methods of comparisons are possible, yet will have even larger uncertainties than those described above. Comparisons with *in situ* observations of surface reflectance are complicated by: (1) spectral differences between *in situ* and GOES sensors, (2) spatial inhomogeneities, considering the different sensor footprints, and (3) angular differences between the sensing systems. In the following, surface reflectance and optical depth retrievals are analysed by the two methods proposed above.

3. Evaluation by comparing surface reflectance retrievals

Comparing satellite observations with those from the surface requires collocating the measurements in both space and time. This ensures that both systems are observing the same aerosol. Spatially, GOES pixels within ± 2 pixels of the AERONET site are averaged (i.e. 5×5 pixels totalling $20 \times 20\,km^2$ excluding clouds). Temporally, the closest AERONET observation is used, limited to a 30 min difference from the GOES observation. Also, a matchup requires at least 10 cloud-free pixels within the 5×5 pixel area to reduce the risk of cloud contamination. Limits are also placed on the spatial variance of τ_G to further reduce possible cloud contamination and ensure that both GOES and AERONET are observing the same aerosol (that is, by removing spatially inhomogeneous aerosol). The AERONET sites which provide data for the matchups from 2001 are listed in table 1.

3.1 *Analysis for AERONET sites*

The instantaneous surface reflectance, $\rho_{sfc,AER}$, is retrieved in an identical manner to that used to retrieve the surface reflectance from the composite clear reflectance ($\rho_{sat,CCR}$) except that an AERONET observation of aerosol optical depth (τ_A) is used. In figure 2(*a*), a time series of $\rho_{sfc,CCR}$ (with varying CCR lengths) and $\rho_{sfc,AER}$ at Goddard Space Flight Center (GSFC) AERONET site for 14:45 UTC is provided. The general trend depicts a seasonal cycle, with higher reflectances in the winter and lower reflectances in the summer. The shortest CCR (7 days) shows spikes in ρ_{sfc} (black line figure 2(*a*)) which are caused by a lack of cloud-free (and/or aerosol-free) observations. This results in spuriously large surface reflectance retrievals, which do not appear with longer composite time period. Also, the surface reflectance is always lower for longer CCR lengths. This is particularly noticeable during September and October where the ρ_{sfc} from the 28-day composite (red line) is much less than that from the 7-day composite (black line).

The scatter between the two reflectances depends on the CCR length and the assumed τ_b. Comparisons of $\rho_{sfc,CCR}$ (for CCR = 14 days and $\tau_b = 0.04$) with $\rho_{sfc,AER}$ from the GSFC AERONET site for 14:45 UTC and all times are provided in figure 2(*b*) and (*c*). The rms. differences for both comparisons are ~ 0.03. Bias and

Table 1. List of AERONET sites used in this study, with location, site principal investigator (PI) and average surface reflectance ($\overline{\rho_{sfc,aer}}$).

Site	Latitude	Longitude	Site PI	$\overline{\rho_{sfc,aer}}$
BONDVILLE	40.05	−88.37	Brent Holben	0.082
Bratts Lake	50.28	−104.70	Bruce McArthur	0.129
BSRN BAO Boulder	40.04	−105.01	Brent Holben	0.132
Cart Site	36.61	−97.41	Mary Jane Bartholomew	0.125
CARTEL	45.38	−71.93	Norm O'Neill	0.090
Chequamegon	45.93	−90.25	Brent Holben	0.069
COVE	36.90	−75.71	Brent Holben	0.020
Dry Tortugas	24.60	−82.80	Ken Voss	0.031
Egbert	44.23	−79.75	Norm O'Neill	0.092
GISS	40.80	−73.96	Brent Holben	0.074
GSFC	39.03	−76.88	Brent Holben	0.072
Harvard Forest	42.53	−72.19	Brent Holben	0.068
Howland	45.20	−68.73	Brent Holben	0.068
KONZA EDC	39.10	−96.61	David Meyer	0.094
Lochiel	49.03	−122.60	Brent Holben	0.071
Maryland Science Center	39.28	−76.62	Brent Holben	0.086
Missoula	46.92	−114.08	Wei Min Hao	0.109
Mont Joli	48.64	−68.16	Brent Holben	0.024
Oyster	37.29	−75.93	Brent Holben	0.082
Pennsylvania State University	40.74	−78.08	Brent Holben	0.074
Philadelphia	40.04	−75.00	Brent Holben	0.093
Rimrock	46.49	−116.99	Brent Holben	0.154
Rochester	44.23	−77.59	Brent Holben	0.095
SERC	38.88	−76.50	Jay Herman	0.074
Sevilleta	34.35	−106.89	Doug Moore	0.182
Sioux Falls	43.74	−96.63	Gregory Stensaas	0.100
Walker Branch	35.96	−84.29	Brent Holben	0.067

rms. differences are provided for all CCR lengths in each figure. Cloud (and possible aerosol) contamination for the 7-day composite is apparent in the elevated rms. values and negative bias. Also, there is some variation in $\rho_{sfc,CCR}$: when varying τ_b from 0.02 to 0.08, ρ_{sfc} changes by (at most) 0.006 (about 5%). In general, the 14-day CCR for GSFC has the lowest bias and rms. values. Results of comparisons at GSFC are similar to those at other sites.

The comparisons of $\rho_{sfc,CCR}$ with $\rho_{sfc,AER}$ for all sites during 2001 are summarized in tables 2 and 3. Again, the rms. and bias errors are largest for the 7-day composite. From the rms. errors, one concludes that: (1) there is little change in rms. between 14 and 28 days, and (2) there is little to no difference in rms. for different τ_b values. The bias, however, shows some variation. The bias is similar in magnitude for CCRs of 14 days and above. This corresponds to a decrease in $\rho_{sfc,CCR}$ as CCR length increases; which occurs because more observations provide more opportunity for a darker observation to occur. Also, changing τ_b has a more noticeable effect on the bias than the rms.; in general, the change in $\rho_{sfc,CCR}$ is ~0.004 or less when changing τ_b from 0.02 to 0.08. In summary, the optimal CCR is near 14 days long with less dependence on τ_b.

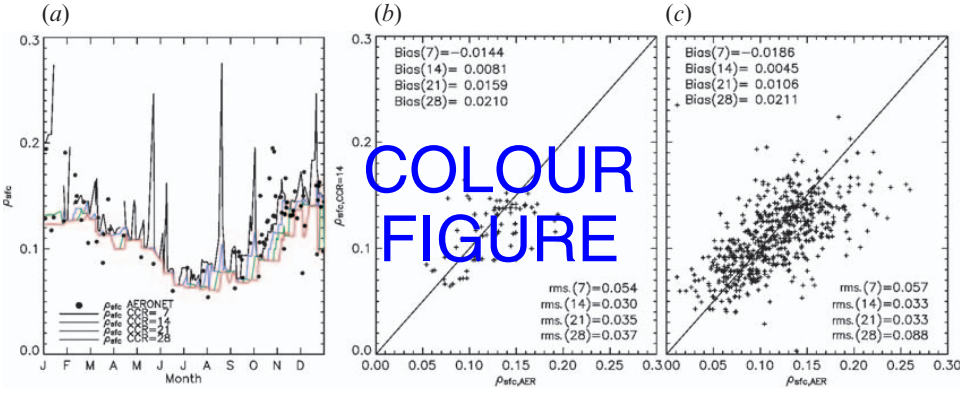

Figure 2. (*a*) Time series of daily surface reflectances at 14:45 UTC for the GSFC AERONET site. Solid lines represent the composite clear reflectance-derived reflectance while dots represent reflectances derived using AERONET τ observations (*b*) $\rho_{sfc,CCR}$ from 14 days versus $\rho_{sfc,AER}$ for 14:45 UTC observations at GSFC. (*c*) $\rho_{sfc,CCR}$ from 14 days versus $\rho_{sfc,AER}$ for all observations at GSFC. The solid line in (*b*) and (*c*) is the one-to-one line.

International Journal of Remote Sensing res60776.3d 15/4/05 15:06:37
The Charlesworth Group, Wakefield +44(0)1924 369598 - Rev 7.51n/W (Jan 20 2003)

4. Evaluation by comparing aerosol optical depth retrievals

Aerosol optical depth is retrieved using the 6S radiative transfer model where the τ_G (at 0.55 μm) is retrieved from a GOES observation (ρ_{sat}), surface reflectance ($\rho_{sfc,CCR}$) and τ_b, such as noted in equation (6) (except in cases of snow). For this step, the primary uncertainty is the assumed aerosol optical properties. Again, the continental aerosol model defined in Lenoble and Brogniez (1984) is used to retrieve aerosol optical depth. This is adequate for evaluation purposes, herein, for three reasons.

First, aerosol model errors will primarily affect the linear slope between τ_G and τ_A, because errors relating to optical properties are generally proportional to τ (Fraser *et al.* 1984, Knapp *et al.* 2002). Also, Knapp (2002) showed that the continental aerosol model matched the aerosol signal observed over the US for most of the AERONET sites investigated.

Second, Zhao *et al.* (2002) relate the linear regression offset (i.e. bias) to calibration and surface errors and the linear slope to aerosol optical property errors. Thus, errors in the aerosol optical property assumptions will have only a small effect on analysis of the linear regression intercept (which is used below to evaluate the removal of the surface effect).

Third, using the continental model is not too different from previous studies. The Global Aerosol Data Set (Koepke *et al.* 1997, Hess *et al.* 1998) provides a climatological spatial aerosol distribution, and describes the aerosol over the US

Table 2. rms. differences between $\rho_{sfc,CCR}$ and $\rho_{sfc,AER}$ for all AERONET sites for various composite lengths (CCR) (in days) and assumed background aerosol optical depths (τ_b).

τ_b	0.02	0.04	0.08
CCR=7	0.067	0.067	0.034
CCR=14	0.034	0.034	0.034
CCR=21	0.030	0.030	0.032
CCR=28	0.030	0.031	0.033

Table 3. Bias ($\rho_{sfc,CCR} - \rho_{sfc,A}$) values for comparison of ρ_{sfc} retrievals for all AERONET sites.

τ_b	0.02	0.04	0.08
CCR=7	−0.022	−0.021	−0.020
CCR=14	0.001	0.002	0.006
CCR=21	0.007	0.009	0.014
CCR=28	0.011	0.013	0.017

primarily as continental. The Moderate Resolution Imaging Spectro-radiometer (MODIS) aerosol algorithm over land (Kaufman *et al.* 1997) uses a continental aerosol model for North America east of 100° W longitude. While the MODIS algorithm tests for the presence of large aerosol, an aerosol model is assumed when none is found. Thus using a simple continental aerosol model will suffice in determining whether the surface effect is removed (that is, if the linear regression intercept is near zero).

The comparison of τ_A with τ_G for GSFC (using a 7-day CCR and τ_b=0.02) is provided in figure 3. The histogram (figure 3(*b*)) shows retrievals of τ as large as 1.0 and the linear regression correlation (figure 3(*a*)) is 0.845 with an rms. difference of 0.12. Negative τ_G values are possible because ρ_{sat} can be lower than the composite (primarily when ρ_{sat} is the darkest pixel in the time period and $\rho_{sat\text{-}CCR}$ is from the second darkest pixel). The retrieval error ($\tau_G - \tau_A$) shows little bias with respect to time of year (figure 3(*c*)) or time of day (figure 3(*d*)). Retrievals using the four CCR lengths (from 7 to 28 days) and three τ_b values are discussed below.

The optimal CCR is determined for the GSFC site from analysis of the linear regression intercepts, which are provided in table 4. Overall, the intercept increases with CCR length and τ_b. For longer composite lengths, the change in intercept is caused by more chances for darker observations, causing surface reflectances to be biased low and increasing the τ_G retrievals. For τ_b, increasing intercepts are caused by more of ρ_{sat} attributed to the atmosphere and less to the surface, resulting in lower retrieved ρ_{sfc} and larger τ_G. The optimal CCR length is 7 days with $0.02 < \tau_b < 0.04$. For other CCR lengths, the τ_b is less than 0.02. However, as will be shown, the optimal CCR length varies in space and time.

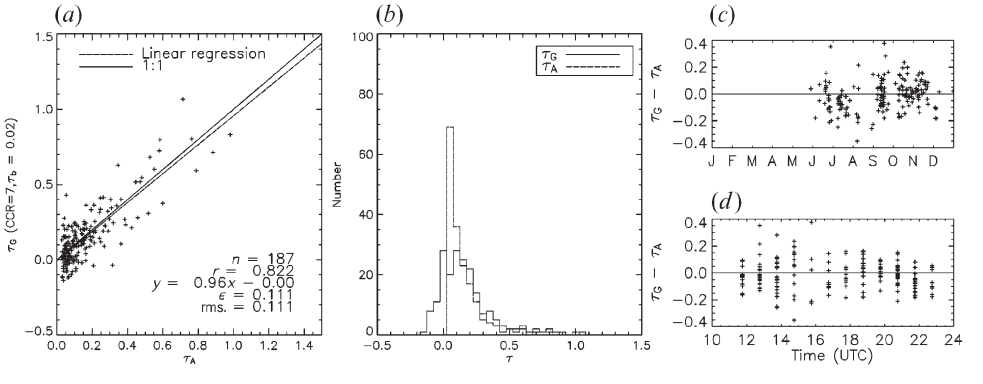

Figure 3. (*a*) Scatter plot for the comparison of τ_G (retrieved using CCR=7 days and τ_b=0.02) with τ_A from GSFC. (*b*) Histograms for τ_G and τ_A. (*c*) Retrieval error (i.e. $\tau_G - \tau_A$) as a function of time of year. (*d*) Retrieval error as function of time of day (UTC).

Table 4. Linear regression intercept for the GSFC τ comparison for varying CCR lengths and τ_b values.

τ_b	0.02	0.04	0.08
CCR=7	−0.004	0.012	0.049
CCR=14	0.066	0.084	0.116
CCR=21	0.098	0.116	0.149
CCR=28	0.113	0.127	0.157

It should be noted that minimizing the linear regression offset (through an optimal CCR/τ_b combination) has a beneficial side effect: it reduces the calibration uncertainty. According to Zhao *et al.* (2002) the retrieval error due to instrument calibration uncertainty is minimized when minimizing the linear regression offset between observed and retrieved optical depths. Thus, by determining an optimal CCR and τ_b herein, the calibration error is minimized.

The linear regression statistics of the τ comparison for all sites are provided in table 5 for combinations of CCR length and τ_b. An example comparison for the 14-day CCR with τ_b=0.02 is shown in figure 4(*a*). The number of matchups (*n*) varies in table 5 with CCR length and τ_b because longer composite time periods have more valid ρ_{sfc} retrievals (this can be seen in figure 2(*a*); note the gaps and spikes in ρ_{sfc} from the 7-day composites compared with longer time periods). The intercept increases with CCR length and τ_b. However, the optimal CCR–τ_b combination has changed. In the ρ_{sfc} comparison, the 14-day CCR had the lowest bias (cf. table 3). For the τ comparison, the optimal composite lengths are 7 days (with $0.04<\tau_b<0.08$) or 14 days (with $\tau_b<0.02$). This apparent variation in CCR length is likely caused by seasonal variation in the surface reflectance.

The rms. and intercept values in table 5 are separated by season in tables 6 and 7, respectively (too few matchups occur in winter for meaningful results). For one CCR length, there is a significant change in bias from summer to autumn. In fact, the intercept nearest zero occurs for CCR=21, 21 and 7 days for spring, summer and autumn, respectively. The seasonal dependence of CCR length derives from the

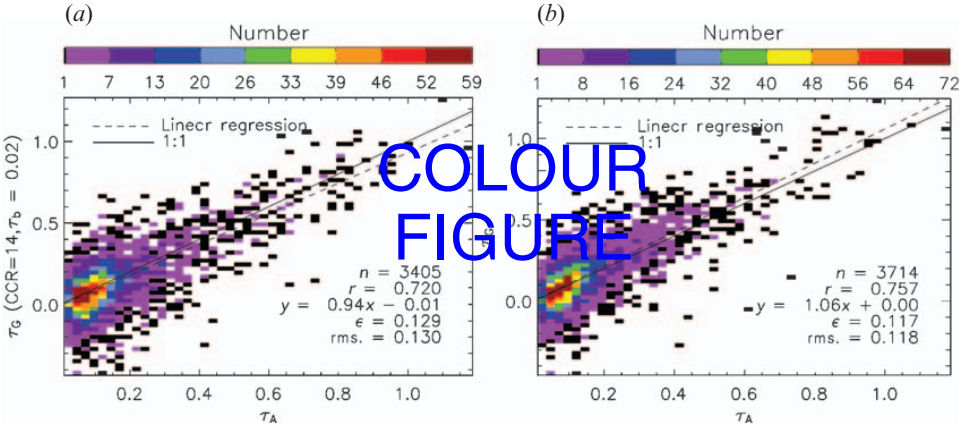

Figure 4. (*a*) Comparison of GOES-retrieved (from the 14-day CCR and τ_b=0.02) with AERONET observations (both at 0.55 μm) as a two-dimensional histogram with linear regression coefficients provided (*b*). Same as (*a*) except using optimal CCR and τ_b according to season (see text). Note the higher correlation and lower noise in (*b*).

Table 5. Linear regression results for τ comparisons for all sites. Summary statistics include number of matchups (*n*), linear regression correlation (*r*), slope (*m*), offset (*b*), and rms. difference between τ_G and τ_A.

CCR	τ_b	n	r	m	b	rms.
7	0.02	3338	0.723	0.950	−0.024	0.134
7	0.04	3405	0.720	0.937	−0.006	0.130
7	0.08	3517	0.723	0.924	0.026	0.127
14	0.02	3472	0.677	0.922	0.028	0.127
14	0.04	3528	0.671	0.907	0.046	0.129
14	0.08	3592	0.658	0.876	0.076	0.137
21	0.02	3764	0.683	0.906	0.070	0.136
21	0.04	3805	0.682	0.900	0.085	0.141
21	0.08	3827	0.673	0.878	0.113	0.154
28	0.02	3833	0.693	0.914	0.089	0.147
28	0.04	3858	0.693	0.908	0.103	0.153
28	0.08	3834	0.684	0.893	0.130	0.169

Table 6. rms. of the τ comparisons for all sites by season.

	Spring			Summer			Autumn		
τ_b	0.02	0.04	0.08	0.02	0.04	0.08	0.02	0.04	0.08
CCR=7	0.131	0.126	0.123	0.153	0.145	0.132	0.121	0.120	0.126
CCR=14	0.119	0.118	0.121	0.126	0.121	0.119	0.133	0.140	0.157
CCR=21	0.119	0.120	0.128	0.116	0.116	0.123	0.161	0.170	0.191
CCR=28	0.128	0.132	0.143	0.121	0.123	0.136	0.178	0.187	0.208

International Journal of Remote Sensing res60776.3d 15/4/05 15:06:38
The Charlesworth Group, Wakefield +44(0)1924 369598 - Rev 7.51n/W (Jan 20 2003)

temporal trend of the surface reflectance. During spring, ρ_{sfc} is decreasing for most sites. Using a long CCR length allows more opportunities to observe a cloudless, low-burden day but any noise (which would cause spuriously low ρ_{sfc}) has less effect since ρ_{sfc} is decreasing seasonally. Thus, the optimal CCR length is around 21 days. Similarly, the surface changes little in the summer. So, the optimal CCR length remains 21 days. In autumn, however, the surface reflectance begins increasing. So for a long CCR, the surface reflectance from the darkest observation (which is likely from the earlier part of the CCR time period) is much different from the surface reflectance when ρ_{sat} is observed (cf. varying CCR lengths in figure 2(*a*)). Thus, the optimal CCR is shorter: 7 days (cf. table 7).

Combining the seasonally-derived optimal CCR–τ_b combinations also increases the correlation between τ_A and τ_G. The retrieval matchups using the optimal combinations (CCR=21, τ_b=0.02 for spring and summer; CCR=7, τ_b=0.02 for autumn) are provided in figure 4(*b*). The change in *n* from figure 4(*a*) is due to the

Table 7. Linear regression intercept of the τ comparisons by season.

	Spring			Summer			Autumn		
τ_b	0.02	0.04	0.08	0.02	0.04	0.08	0.02	0.04	0.08
CCR=7	−0.051	−0.035	−0.013	−0.088	−0.069	−0.032	0.004	0.023	0.056
CCR=14	−0.029	−0.014	0.008	−0.035	−0.017	0.015	0.073	0.091	0.123
CCR=21	−0.004	0.009	0.031	0.004	0.019	0.051	0.116	0.131	0.164
CCR=28	0.015	0.029	0.053	0.029	0.043	0.074	0.138	0.152	0.181

change in CCR lengths and τ_b. In particular, the bias (i.e. linear regression offset) decreases from -0.01 to near zero. Also, the correlation increases and the noise decreases.

It should be noted that in spite of the simplistic assumption of the aerosol model, optical depth estimates agree well with observations. The optimal combination (figure 4(*b*)) results in a bias (i.e. linear regression intercept) near zero and a slope within 6% of 1. This is consistent with Knapp (2002) who found that the continental aerosol model closely matched the aerosol signal detected at AERONET sites. Certainly, improvements could be made to allow the aerosol model to vary, but this initial result shows that the rms. errors are near 0.12 and the correlation coefficient is 0.76.

Given this accuracy, two examples of aerosol retrievals are provided which show aerosol events in and around the US. The aerosol product from 16:15 UTC on 26 June 2002 is provided in figure 5. The areas in colour (ranging from blue through red) depict aerosol optical depth while grey-scale portions depict reflectance of clouds (as determined from the cloud mask). There are three large aerosol plumes present, which are believed to be the following based on comparison with the Navy Aerosol Analysis and Prediction System optical depth forecast for that day: Saharan dust in the Caribbean, industrial aerosol in the mid-Atlantic region, and smoke from a forest fire in Manitoba transported to New Brunswick (Canada). It should also be noted that while the method is primarily designed and validated (herein) to estimate surface reflectance of land, the assumptions used are entirely appropriate for use over ocean. In particular, the assumptions that the surface reflectance changes slowly in time (one could argue the surface reflectance in the open ocean is constant)

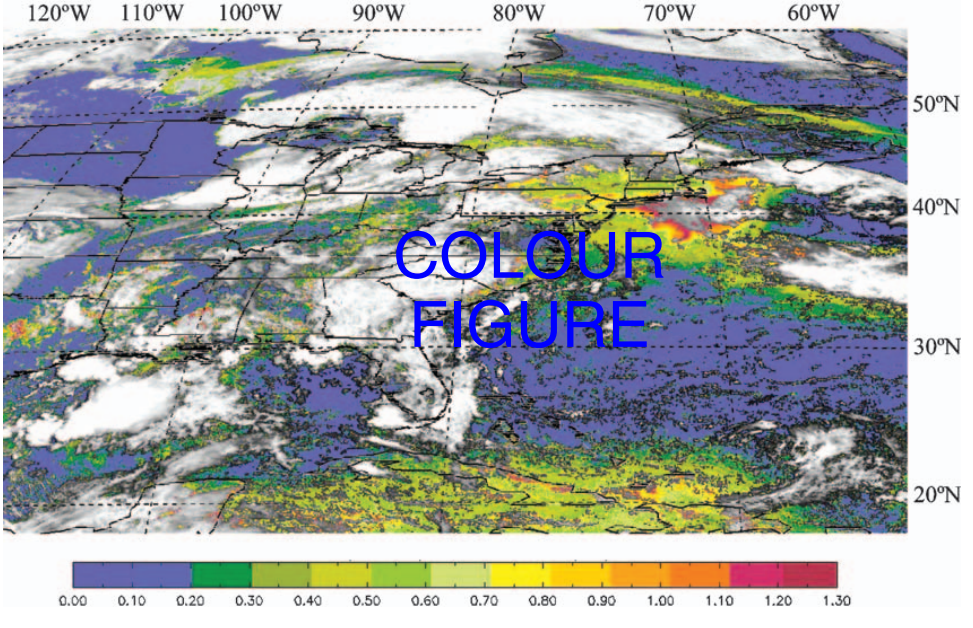

Figure 5. Example of the GOES τ retrieval for 26 June 2002 at 16:15 UTC over the eastern US depicting three distinct aerosol plumes: Saharan dust in the Caribbean, industrial aerosol in the mid-Atlantic region and forest fire smoke plume stretching from Manitoba to New Brunswick (Canada).

and that it is Lambertian (we avoid areas of specular reflection) are accurate when used appropriately.

The second example provides a preliminary comparison with MODIS retrievals. The MODIS instrument was first launched on the Earth Observing System (EOS)–Terra satellite in December 1999 with a primary goal to provide better understanding of the aerosol distribution. For retrievals over land, ρ_{sat} at 2.2 μm is used to estimate the surface contribution to the blue and red visible-wavelength channels (the 0.45 and 0.66 μm channels). While an aerosol climatology provides the aerosol optical properties for the retrieval, it also uses spectral observations to estimate fraction of dust. The MODIS aerosol optical depth over land algorithm retrieves aerosol optical depth to within $0.05+0.2\tau$ (Kaufman *et al.* 1997) which has been verified with MODIS airborne simulator measurements (Chu *et al.* 1998). The aerosol retrieval over ocean uses a separate algorithm because the ocean reflectance (in most cases) is better characterized than land. Therefore, the aerosol optical depth—along with properties derived from the spectral reflectance such as size—are derived in the MODIS τ retrieval algorithm for water with an expected uncertainty of less than $0.05+0.05\tau$ (Tanré *et al.* 1997). The MODIS aerosol data used herein are from the Level 2 processing, which is compared with the GOES τ retrieval.

The MODIS aerosol optical depth (at 0.55 μm) along the eastern US from 9 August 2001 at 16:15 UTC (actual swath time is 16:10–16:20 UTC) is shown in figure 6(*a*). The data gap along the East Coast represents the Sun glint portion of the image scan where aerosol optical depth retrievals are unavailable. The other irregularly shaped gaps are regions of cloud cover. The corresponding GOES τ retrieval image (at 16:45 UTC on the same day) is shown in figure 6(*b*). Both retrievals show a plume of aerosol near Virginia extending over the Atlantic (likely from industrial pollution) and a second plume in the Caribbean (likely desert dust from the Sahara). Quantitatively (figure 7), the comparisons show an overall rms. difference of 0.12, which is well within the range of rms. values observed at AERONET sites (shaded regions of figure 7 are the estimated error level of $\Delta\tau = \pm 0.2 \pm 0.2\tau$ (Knapp *et al.* 2002)). Separating land retrievals from ocean shows that the large noise comes from the land areas (rms.=0.13) compared to oceans (rms.=0.08). Thus, τ retrieved from the GOES imager compares well with τ retrieved from MODIS.

It is interesting to again note the high correlation and low noise in spite of the simplistic assumption that the aerosol is continental. In figure 6, the two aerosol plumes are likely very different: small sulphate aerosol over the mid-Atlantic and large Saharan dust over the Caribbean. Thus, it would be expected that the MODIS retrieval would show systematic differences because the MODIS algorithm varies the optical properties to match the spectral signature (as opposed to the fixed aerosol model in the GOES algorithm). However, the ocean comparison shows little bias difference with both slope and offset near optimal values. Thus, in this case, GOES aerosol optical depth compares well with that retrieved from MODIS.

5. Conclusions

In addition to their impact on climate, aerosols have significant health and aviation impacts, which are particularly sensitive to large concentrations of aerosols. Observing aerosols from GOES would allow high temporal sampling important in these cases. However, retrieving aerosol optical depth from GOES imagery requires

109915

International Journal of Remote Sensing res60776.3d 15/4/05 15:06:44
The Charlesworth Group, Wakefield +44(0)1924 369598 - Rev 7.51n/W (Jan 20 2003)

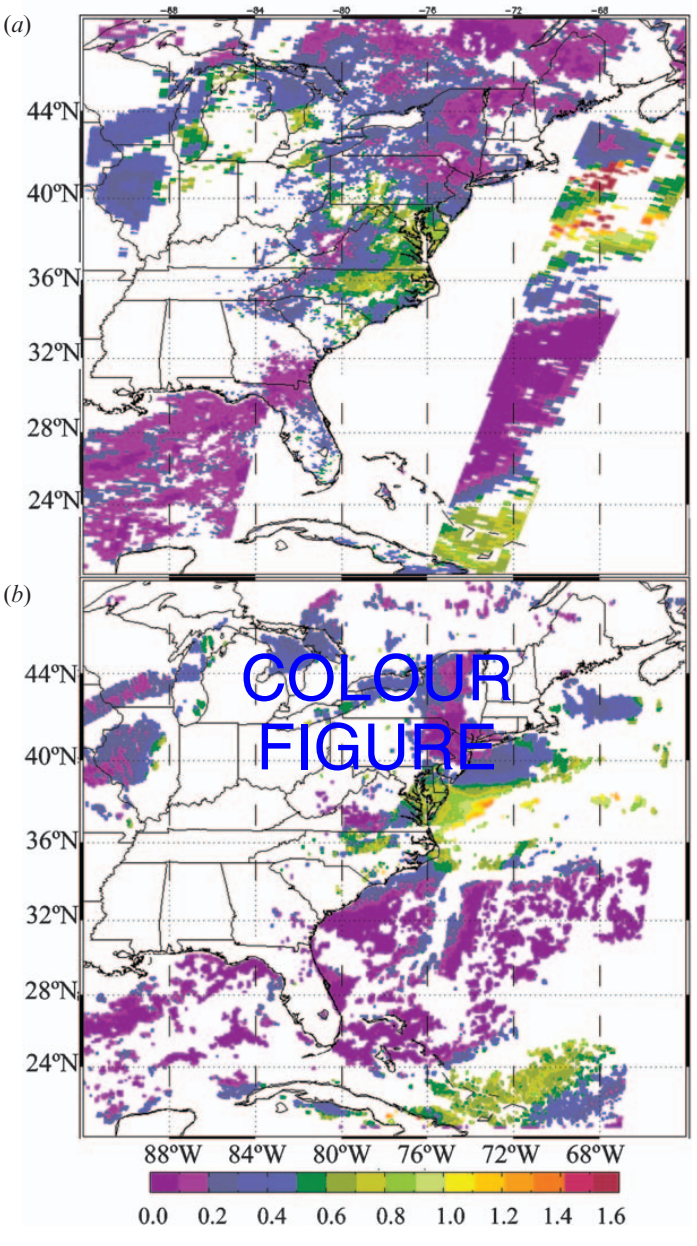

Figure 6. Retrieved aerosol optical depth from (*a*) MODIS and (*b*) GOES-8 on 9 August 2001 at 16:15 UTC (MODIS) and 16:45 UTC (GOES). Note the aerosol plume in the mid-Atlantic states (and nearby ocean) and in the Caribbean. Also, note the continuity in the τ_G for the coastal mid-Atlantic and the Great Lakes region.

estimation of the surface contribution to the TOA detected reflectance. This paper details how the surface reflectance can be estimated for portions of the North American continent using temporal composites of visible imagery. The surface reflectance estimates are validated in two ways: by comparing with more accurate ρ_{sfc} retrievals (when τ is known from AERONET observations) and from aerosol optical depth retrieval validation using AERONET. In particular, the second

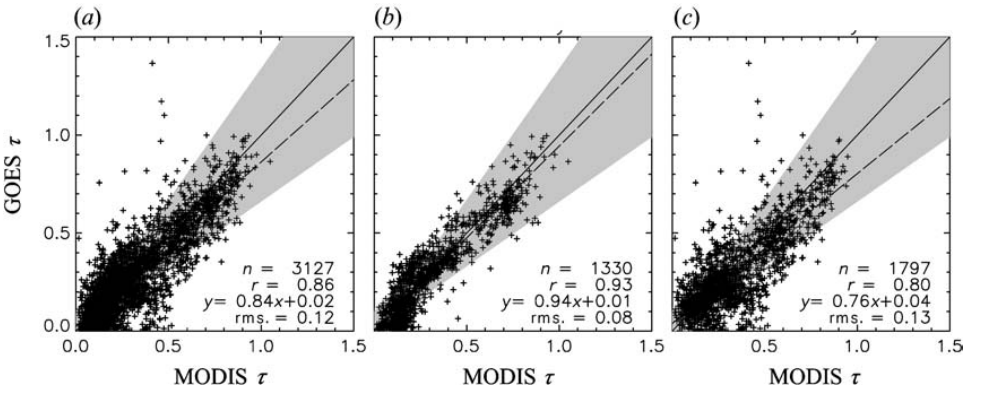

Figure 7. Comparison of GOES τ with MODIS τ for the data shown in figure 6, for (*a*) all matchups and separated by (*b*) ocean and (*c*) land (since a separate MODIS algorithm exists for each). The larger scatter (i.e. rms.) over land is likely due to differences in aerosol models, surface reflectance estimates and cloud masks (solid and dashed lines are the 1–1 relationship and the linear regression, respectively).

evaluation method is important because it is sensitive to surface errors and it is the purpose for this study.

In the first method, ρ_{sfc} from the composite clear reflectance is compared with ρ_{sfc} retrieved using *in situ* observations from AERONET. This analysis yields an estimate of rms. difference for the CCR method of about ± 0.02 to ± 0.04 depending on the surface reflectance. An optimal CCR–τ_b combination is difficult to detect given the small variations in rms. and bias with respect to τ_b. Since this method had uncertainty related to the retrieval and ground data (i.e. $\rho_{sfc,AER}$), another method was also used to evaluate the results.

In the second method, the ability to separate the surface component from the atmospheric component is further analysed by evaluating the retrieved optical depths using the CCR-derived surface reflectances. This approach is more sensitive to variations in CCR–τ_b than was the ρ_{sfc} analysis. When comparing τ retrievals at all sites (for all times of year), the optimal CCR–τ_b combination is around 14 days with τ_b=0.02. Yet, seasonal variation in surface reflectance causes a seasonal variation in the optimal CCR length, with a shorter length during autumn and a longer CCR during spring and summer. By varying the CCR length through the year, the separation of the surface from the atmospheric component is more accurate, which is measured through increased correlation between observed and retrieved aerosol optical depths and less bias between the two (i.e. linear regression intercept values closer to zero).

Given that Knapp (2002) determined that an aerosol signal exists in GOES visible data for most regions of North America and that this study shows that the surface contribution can be accurately removed, it is possible to retrieve aerosol optical depths over much of North America. This retrieval method does not depend on ground measurements, but used comparisons with AERONET to demonstrate the retrieval accuracy. Two preliminary examples of aerosol retrievals were provided, including a comparison with the MODIS product.

Admittedly, the assumptions in this approach could be improved. For instance, one might use bidirectional reflectance information derived from MODIS or the Polarization and Directionality of Earth's Reflectances (POLDER) observations to

replace the Lambertian assumption. Also, the aerosol model could be varied given input from computer simulations (for case studies), forecasts or observations from other satellites like MODIS (for real-time application). And while the τ_b is empirically derived here, one might determine it more accurately using long-term analyses of AERONET sites.

Nonetheless, the results showed surprisingly good correlations in the ensuing τ retrievals. Particularly, by varying the CCR length during the year, the rms. differences with AERONET are only 0.12 with correlations near 0.76. And in spite of the simplistic aerosol model used herein, linear regression correlations and slopes were near optimal. A similar result was found in comparing the τ_G with τ retrieved from MODIS. Future work should investigate more comparisons with MODIS, vary the aerosol optical properties, and look at diurnal aspects of the retrieval performance. While a drawback of these results is the large scatter at low optical depths suggesting an inability to sense low aerosol optical depths, the retrieval method should prove useful for detecting large-scale aerosol episodes such as dust outbreaks, industrial pollution and biomass burning. This aspect should not be overlooked when evaluating the adequacy of GOES for aerosol monitoring because these events are important to air quality, aviation and hazard management.

Acknowledgments

The authors acknowledge numerous people that have made this research possible through the provision of data. Cindy Combs of CIRA was instrumental by providing access to data after a system failure. Andy Heidinger's advice concerning cloud masking was valuable. The AERONET is an invaluable resource for this work, therefore we are grateful to Brent Holben and the AERONET staff, and the principal investigators listed in table 1 for making their AERONET data available for this research as well as the AEROCAN/AERONET network (PIs Norm O'Neill and Alain Royer). Also, thanks to Peter Romanov for providing access to the GOES data. Finally, this work was supported by the NOAA/GIMPAP and the NASA/ Global Aerosol Climatology Project (purchase order S-10189X, Michael Mishchenko, Project Scientist).

References

Bergin, M.H., Cass, G.R., Xu, J., Fang, C., Zeng, L.M., Yu, T., Salmon, L.G., Kiang, C.S., Tang, X.Y., Zhang, Y.H. and Chameides, W.L., 2001, Aerosol radiative, physical, and chemical properties in Beijing during June 1999. *Journal of Geophysical Research*, **106**, pp. 17 969–17 980.

Charlson, R.J., Langner, J., Rodhe, H., Leovy, C.B. and Warren, S.G., 1991, Perturbation of the northern hemisphere radiative balance by backscattering from anthropogenic sulfate aerosols. *Tellus*, **43AB**, pp. 152–163.

Chu, D.A., Kaufman, Y.J., Remer, L.A. and Holben, B.N., 1998, Remote sensing of smoke from MODIS airborne simulator during the SCAR-B experiment. *Journal of Geophysical Research*, **103**, pp. 31 979–31 987.

Fraser, R.S., Kaufman, Y.J. and Mahoney, R.L., 1984, Satellite measurements of aerosol mass and transport. *Atmospheric Environment*, **18**, pp. 2577–2584.

Gebhart, K.A., Copeland, S. and Malm, W.C., 2001, Diurnal and seasonal patterns in light scattering, extinction and relative humidity. *Atmospheric Environment*, **35**, pp. 5177–5191.

Haywood, J. and Boucher, O., 2000, Estimates of the direct and indirect radiative forcing due to tropospheric aerosols: a review. *Reviews of Geophysics*, **38**, pp. 513–543.

HAYWOOD, J.M., RAMASWAMY, V. and SODEN, B.J., 1999, Tropospheric aerosol climate forcing in clear-sky satellite observations over the oceans. *Science*, **283**, pp. 1299–1303.

HEGG, D.A., LIVINGSTON, J.M., HOBBS, P.V., NOVAKOV, T. and RUSSELL, P., 1997, Chemical apportionment of aerosol column optical depth off the mid-Atlantic coast of the United States. *Journal of Geophysical Research*, **102**, pp. 25293–25303.

HERMAN, B.M. and BROWNING, S.R., 1975, The effect of aerosols on the Earth-atmosphere albedo. *Journal of Atmospheric Science*, **32**, pp. 1430–1445.

HESS, M., KOEPKE, P. and SCHULT, I., 1998, Optical Properties of Aerosols and Clouds: the software package OPAC. *Bulletin of the American Meteorological Society*, **79**, pp. 831–844.

HOLBEN, B.N., ECK, T.F., SLUTSKER, I., TANRÉ, D., BUIS, J.P., SETZER, A.W., VERMOTE, E.F., REAGAN, J.A., KAUFMAN, Y.J., NAKAJIMA, T., LAVENU, F., JANKOWIAK, I. and SMIRNOV, A., 1998, AERONET—a federated instrument network and data archive for aerosol characterization. *Remote Sensing of the Environment*, **66**, pp. 1–16.

IPCC, 2001, *Climate Change 2001: The Scientific Basis* (New York: Cambridge University Press).

KAUFMAN, Y.J. and REMER, L.A., 1994, Detection of forests using mid-IR reflectance: an application for aerosol studies. *IEEE Transactions on Geoscience and Remote Sensing*, **32**, pp. 672–683.

KAUFMAN, Y.J., TANRÉ, D., REMER, L.A., VERMOTE, E.F., CHU, A. and HOLBEN, B.N., 1997, Operational remote sensing of tropospheric aerosol over land from EOS moderate resolution imaging spectroradiometer. *Journal of Geophysical Research*, **102**, pp. 17051–17067.

KAUFMAN, Y.J., HOLBEN, B.N., TANRÉ, D., SLUTSKER, I., SMIRNOV, A. and ECK, T.F., 2000, Will aerosol measurements from Terra and Aqua polar orbiting satellites represent the daily aerosol abundance and properties? *Geophysical Research Letters*, **27**, pp. 3861–3864.

KAUFMAN, Y.J., TANRÉ, D. and BOUCHER, O., 2002, A satellite view of aerosols in the climate system. *Nature*, **419**, pp. 215–223.

KING, M.D., KAUFMAN, Y.J., TANRÉ, D. and NAKAJIMA, T., 1999, Remote sensing of tropospheric aerosols from space: past, present and future. *Bulletin of the American Meteorological Society*, **80**, pp. 2229–2259.

KNAPP, K.R., 2002, Quantification of aerosol signal in GOES-8 visible imagery over the U.S. *Journal of Geophysical Research*, **107**, 10.1029/2001JD002001.

KNAPP, K.R. and VONDER HAAR, T.H., 1999, Calibration of the Eighth Geostationary Observational Environmental Satellite (GOES-8) Imager Visible Sensor. *Journal of Atmospheric and Oceanic Technology*, **17**, pp. 1639–1644.

KNAPP, K.R., VONDER HAAR, T.H. and KAUFMAN, Y.J., 2002, Aerosol optical depth retrieval from GOES-8: uncertainty study and retrieval validation over South America. *Journal of Geophysical Research*, **107**, 10.1029/2001JD000505.

KOEPKE, P. and QUENZEL, H., 1979, Turbidity of the atmosphere determined from satellite: calculation of optimum viewing geometry. *Journal of Geophysical Research*, **84**, pp. 7847–7856.

KOEPKE, P., HESS, M., SCHULT, I. and SHETTLE, E.P., 1997, Global Aerosol Data Set, Max Planck Institute for Meteorologie, Hamburg.

LENOBLE, J. and BROGNIEZ, C., 1984, A comparative review of radiation aerosol models. *Beiträge zur Physik de Atmosphäre*, **57**, pp. 1–20.

MCCLATCHEY, R.A., FENN, R.W., SELBY, J.E.A., VOLZ, F.E. and GARING, J.S., 1972, Optical properties of the atmosphere. AFCRL-TR-71-0279, Bedford, MA.

PEPPLER, R.A., BAHRMANN, C.P., BARNARD, J.C., CAMPBELL, J.R., CHENG, M.-D., FERRARE, R.A., HALTHORNE, R.N., HEILMAN, L.A., HLAVKA, D.L., LAULAINEN, N.S., LIN, C.-J., OGREN, J., POELLOT, M.R., REMER, L.A., SASSEN, K.,

SPINHIRNE, J.D., SPLITT, M.E. and TURNER, D.D., 2000, ARM southern Great Plains site observations of the smoke pall associated with the 1998 Central American fires. *Bulletin of the American Meteorological Society*, **81**, pp. 2563–2591.

PLATNICK, S. and TWOMEY, S., 1994, Remote sensing the susceptibility of cloud albedo to changes in drop concentration. *Atmospheric Research*, **34**, pp. 85–98.

PRINS, E.M., FELTZ, J.M., MENZEL, W.P. and WARD, D., 1998, An overview of GOES-8 diurnal fire and smoke results for SCAR-B and 1995 fire season in South America. *Journal of Geophysical Research*, **103**, pp. 31821–31835.

SMIRNOV, A., HOLBEN, B.N., DUBOVIK, O.V., O'NEILL, N.T., ECK, T.F., WESTPHAL, D.L., GOROCH, A.K., PIETRAS, C. and SLUTSKER, I., 2002, Atmospheric aerosol optical properties in the Persian Gulf. *Journal of Atmospheric Science*, **59**, pp. 620–634.

STOWE, L.L., DAVIS, P.A. and MCCLAIN, E.P., 1999, Scientific basis and initial evaluation of the CLAVR-1 global clear/cloud classification algorithm for the advanced very high resolution radiometer. *Journal of Atmospheric and Oceanic Technology*, **16**, pp. 656–681.

TANRÉ, D., KAUFMAN, Y.J., HERMAN, M. and MATTOO, S., 1997, Remote sensing of aerosol properties over oceans using the MODIS/EOS spectral radiances. *Journal of Geophysical Research*, **102**, pp. 16971–16988.

VERMOTE, E.F., TANRÉ, D., DEUZÉ, J.L., HERMAN, M. and MORCRETTE, J.-J., 1997a, Second simulation of the satellite signal in the solar spectrum, 6S: an overview. *IEEE Transactions on Geoscience and Remote Sensing*, **35**, pp. 675–686.

VERMOTE, E.F., EL SALEOUS, N., JUSTICE, C.O., KAUFMAN, Y., PRIVETTE, J.L., REMER, L.A., ROGER, J.C. and TANRÉ, D., 1997b, Atmospheric correction of visible to middle infrared EOS–MODIS data over land surfaces: background, operational development and validation. *Journal of Geophysical Research*, **102**, pp. 17131–17141.

XU, J., BERGIN, M.H., YU, X., LIU, G., ZHAO, J., CARRICO, C.M. and BAUMANN, K., 2002, Measurement of aerosol chemical, physical and radiative properties in the Yangtze Delta region of China. *Atmospheric Environment*, **36**, pp. 161–173.

ZHANG, J. and CHRISTOPHER, S.A., 2001, Intercomparison of smoke aerosol optical thickness derived from GOES 8 imager and ground-based Sun photometers. *Journal of Geophysical Research*, **106**, pp. 7387–7397.

ZHAO, T.X.-P., STOWE, L.L., SMIRNOV, A., CROSBY, D., SAPPER, J. and MCCLAIN, C.R., 2002, Development of a global validation package for satellite oceanic aerosol optical thickness retrieval based on AERONET observations and its application to NOAA/NESDIS operational aerosol retrievals. *Journal of the Atmospheric Sciences*, **59**, pp. 294–312.

Authors Queries

Journal: **International Journal of Remote Sensing**
Paper: **109915**
Title: **Toward aerosol optical depth retrievals over land from GOES visible radiances: determining surface reflectance**

Dear Author
During the preparation of your manuscript for publication, the questions listed below have arisen. Please attend to these matters and return this form with your proof. Many thanks for your assistance

Query Reference	Query	Remarks
1	IPCC – to be given in full.	
2	Zhang and Christopher 2002 in text, 2001 in References – which date is correct? Knapp et al. 2001 in text, 2002 in References – which date is correct?	
3	figure 2 –reference is made in the text to colour in this figure.	